International Journal of Nanomedicine

Dovepress
open access to scientific and medical research

Open Access Full Text Article

ORIGINAL RESEARCH

Glucose oxidase complexed gold-graphene nanocomposite on a dielectric surface for glucose detection: a strategy for gestational diabetes mellitus

This article was published in the following Dove Press journal:
International Journal of Nanomedicine

Yueping Ge[1]
Thangavel Lakshmipriya[2]
Subash CB Gopinath[2,3]
Periasamy Anbu[4]
Yeng Chen[5]
Firdaus Hariri[6]
Lu Li[7]

[1]Department of Gynaecology and Obstetrics, Henan Provincial People's Hospital, People's Hospital of Zhengzhou University, Zhengzhou City, Henan Province 450003, People's Republic of China; [2]Institute of Nano Electronic Engineering, Universiti Malaysia Perlis, Kangar, Perlis 01000, Malaysia; [3]School of Bioprocess Engineering, Universiti Malaysia Perlis, Arau 02600, Perlis, Malaysia; [4]Department of Biological Engineering, College of Engineering, Inha University, Incheon 402-751, Republic of Korea; [5]Department of Oral & Craniofacial Sciences, Faculty of Dentistry, University of Malaya, Kuala Lumpur 50603, Malaysia; [6]Department of Oral and Maxillofacial Clinical Sciences, Faculty of Dentistry, University of Malaya, Kuala Lumpur 50603, Malaysia; [7]Department of Obstetrics, Jinan Central Hospital Affiliated to Shandong University, Jinan City, Shandong Province 250013, People's Republic of China

Correspondence: Lu Li
Department of Obstetrics, Jinan Central Hospital Affiliated to Shandong University, 105 Jiefang Rd, Lixia Qu, Jinan City, Shandong Province 250013, People's Republic of China
Email lilu2019@sina.com

Background: Gestational diabetes mellitus is a commonly occurring metabolic disorder during pregnancy, affecting >4% of pregnant women. It is generally defined as the intolerance of glucose with the onset or initial diagnosis during pregnancy. This illness affects the placenta and poses a threat to the baby as it affects the supply of proper oxygen and nutrients.
Purpose: Due to the high percentage of affected pregnant women, it should be mandatory to evaluate glucose levels during pregnancy and there is a need for a continuous monitoring system.
Methods: Herein, the investigators modified the interdigitated (di)electrodes (IDE) sensing surface to detect the glucose on covalently immobilized glucose oxidase (GOx) with the graphene. The characterization of graphene and gold nanoparticle (GNP) was performed by high-resolution microscopy.
Results: Sensitivity was found to be 0.06 mg/mL and to enhance the detection, GOx was complexed with GNP. GNP-GOx was improved the sensitive detection twofold from 0.06 to 0.03 mg/mL, and it also displayed higher levels of current changes at all the concentrations of glucose that were tested. High-performance of the above IDE sensing system was attested by the specificity, reproducibility and higher sensitivity detections. Further, the linear regression analysis indicated the limit of detection to be between 0.02 and 0.03 mg/mL.
Conclusion: This study demonstrated the potential strategy with nanocomposite for diagnosing gestational diabetes mellitus.

Keywords: gestational diabetes, glucose oxidase, graphene, interdigitated electrode, gold nanoparticle

Introduction

Gestational diabetes mellitus is the condition of the intolerance glucose level with the onset or the first recognized complication during the pregnancy period.[1,2] Studies have proved that 6–14% of women in West Africa and 13–18% of women in South Asia were affected by the gestational diabetes. Since most cases of the gestational diabetes were found to develop after 24 weeks, oral glucose tolerance test is usually carried out during the period of 24–28 weeks. The gestational diabetes is increasing the risk of hyperbilirubinemia, birth trauma, macrosomia and hypoglycemia.[3] At the same time, the controlled diabetes was achieved with a normal perinatal outcome and does not show any complication. Proper and controlled diet with a continuous monitoring is needed to maintain the normal glucose level.[4–6] Various sensors and sensing surfaces have been used to monitor

the level of glucose.[7–10] Attempts to improve the biosensor are the paramount to detect the target for the particular disease with the lower level, in order to improve the human life quality. Interaction of biomolecule with a high affinity and the sensing surface modification are playing a crucial role to enhance the limit of detection.[11]

Graphene is a zero-gap semiconductor material with electroactive and transparent properties. The application of graphene has spread widely in the fields of solar cell, electrical circuits, sensors, energy and biomedicine.[12,13] Among these, graphene-based biosensing applications in electrochemical, electrochemiluminescence, impedance and fluorescence sensors are welcomed due to its optical, thermal and electrical properties.[14] In particular, graphene is one of the well-established sensing surfaces in electrochemical sensor due to its excellent electron mobility and conductivity.[15–17] Moreover, the larger surface area of graphene extends the immobilization of biomolecules on the sensing area by the covalent linking or the passive adsorption. While the excellent conductivity and small bandgap are congenial for conducting the electron flow between the biomolecular attachment and the electrode surface.[18] In the current study, graphene was modified on interdigitated electrode (IDE), a dielectric sensing surface used to detect the level of glucose by interacting the glucose oxidase (GOx). To improve the sensitivity, GOx was conjugated with gold nanoparticle (GNP) and compared the detection of glucose without conjugation of GNP to GOx.

Nanomaterial application in the field of biosensor has mainly used in two ways. One is for surface modification and other one is the conjugation with the desired molecule to elevate the limit of detection.[19,20] It was proved that nanomaterial-conjugated biomolecules are more stable and enhanced the detection limit.[21] The nanomaterial-conjugated biomolecule makes the proper arrangement of on the sensing surfaces and improves the detection.[22] Among the available nanomaterials, gold displays the optical absorption at infrared and visible wavelengths and it can be tuned by altering the size. In addition, gold can be easily functionalized, high yield in synthesize, more stable with biomolecules, are the interesting characteristics utilized in the field of biosensor. GNP has been used in several ways in biosensor to develop the novel detection strategies. Almost most of the sensors including surface plasmon resonance, Raman spectroscopy, waveguide-mode sensor, colorimetric assay, fluorescence spectroscopy and electrochemical sensor were utilized the gold-based materials to improve the detections.[23–26] GNP-conjugated aptamer or antibody was used in colorimetric assays to detect the smaller molecule by a simple naked eye. The present research was focused on the detection of glucose by utilizing the conjugated GOx and GNP on the graphene-modified IDE surface. This study compared the detection of glucose in the graphene-GOx and graphene-GOx-GNP modified dielectric (IDE) sensing surfaces.

IDE is a powerful sensing strategy, allowing to measure the changes at the liquid/solid interface of the surface-modified electrodes created by the physical, chemical and biological recognitions.[27] IDE sensor allows two electrodes stick infuse and placed each other, consequently the distance between two electrodes is reduced into a smaller size, as a result it shows the better power density and capability. Moreover, the positive features with the rapid kinetic detection, miniature in the desired size and lesser biofouling attract the researchers to apply the IDE to detect wide range of diseases.[27] It was proved that the surface of IDE modified by the carbon and gold materials improved the detection level.[28] Utilizing these proved positive features, the present work focused to monitor the level of glucose interaction on the graphene-GOx and graphene-GOx-GNP modified IDE sensing surfaces.

Materials and methods

Reagents and biomolecules

GOx, glucose and PBS were procured from Sigma-Aldrich (USA). GNP was from Nanocs, USA. Ethanolamine was bought from Fisher Scientific (UK). The control analytes (lactose and fructose) were obtained from Sigma-Aldrich . 16-mercaptoundecanoic acid (16-MUA) and PBS were from Sigma-Aldrich. N-hydroxysuccinimide (NHS) and N-ethyl-N'-(3-dimethylaminopropyl)carbodiimide hydrochloride (EDC) were procured from GE Healthcare (USA). Graphene was synthesized by the procedure outlined by Gopinath et al.[29]

IDE sensing surface fabrication

IDE fabrication was followed as prepared previously using different parameters for the physical modifications on the surface.[30] Silver IDE electrode was overlaid on the silicon wafer (<100>) using the traditional wet etching method. The positive photoresist was coated on the silicon wafer, followed by a soft bake for 90 s. Ultraviolet light exposure was conducted for 10 sto allow the pattern transfer to be done from the

IDE mask onto the surface. After that, the development process was carried for 15 s by using RD-6 developer. Then, the sample was baked at 110°C to remove the unwanted moisture and improve the adhesion between the silver and SiO_2 layer. Finally, the unexposed area was removed using the silver etchant for 23 sand then cleaned with acetone.

Surface analyses of graphene and GNP

The morphology of the fabricated sensor surface was analyzed by scanning electron microscopy and high-power microscopy-assisted 3D-nanoprofiler. In addition, the quality of the nanomaterials attached on IDE surfaces was analyzed under field-emission scanning electron microscopy (FESEM), field-emission transmission electron microscopy (FETEM) and atomic force microscopy (AFM). The basic parameters followed for these analyses were followed as stated in our earlier reports.[31,32] Further, Fourier-transform infrared spectroscopy (FTIR) and zeta potential analyses were performed as described.[31]

Conjugation of GNP with GOx

To immobilize the GNP with GOx, first 16-MUA (5 mM) was mixed with GNP to make the link by the 2-ends (COOH and SH) of 16-MUA. The unbound 16-MUA was eliminated by the centrifugation followed by the addition of 1:1 ratio of 200 mM of EDC and 50 mM of NHS, for activating the COOH to immobilize on amine group of GOX. The activated surface of GNP was mixed with different concentrations of GOx (100–500 nM) to get the final GNP-GOx conjugates.

Immobilization of graphene on the IDE sensing surface

To immobilize the graphene on the IDE sensing surface, first 1 mg of acid-washed graphene was dispersed in 0.25% APTES [3-Aminopropyl)tiethoxysilane] and kept at room temperaturefor 1 hr. Simultaneously, 1% of KOH was dropped on the IDE surface and kept for 5 mins to generate the hydroxyl groups. And then the graphene (dispersed in APTES) was dropped on the KOH activated IDE sensing surface. Immediately, the GOx or GOx-GNP was dropped on the surface to get the final surface of graphene-GOx or graphene-GOx-GNP. The experimental steps outlined by Zheng et al (2013)[33] were considered for the proper immobilization.

Detection of glucose detection on graphene-GOx and graphene-GOx-GNP surfaces: comparative analysis

The glucose detection was compared on graphene-GOx and graphene-GOx-GNP modified surfaces. Before that these surfaces were blocked by 1 M of ethanolamine to avoid the nonspecific interaction of biomolecules. And then 0.5 mg/mL of glucose was dropped on both surfaces to check the interaction of glucose and GOx. The current changes before and after the additions of glucose were noted. To check the limit of detection, different concentrations of glucose (0.03–0.5 mg/mL) were added on both graphene-GOx and graphene-GOx-GNP modified surfaces. The current changes were noticed for each concentration and compared by the voltammetry at the range of 0–2 V.

Specific detection of glucose on graphene surface

For the specific deletion of glucose on the graphene-GOx-GNP modified surfaces, three different control sugar interactions were carried out on the GOx modified surfaces and compared with the genuine target, glucose. The similar concentrations of glucose and the control sugars (lactose and fructose) were dropped independently on the graphene-GOx-GNP modified surfaces, the changes in the current were noted and compared.

Results and discussion

Gestational diabetes is the metabolic disorder happening during the period of pregnancy and the continuous monitoring is mandatory for the normal perinatal outcome. Improved sensing method helps to monitor the glucose level efficiently during the gestational period. The current research has been carried out on the graphene-modified IDE sensing surface for the efficient detection of glucose level. Figure 1 shows the schematic representation of glucose detection on the IDE sensor. As shown in the figure, the surface of IDE modified into graphene-GOx or graphene-GOx-GNP, and then glucose detection was performed to compare on these surfaces.

Morphological observations: nanoscale imaging

Before proceeding to the surface chemical functionalization and the interactive analyses, the graphene and gold materials used for this study were characterized by high-resolution

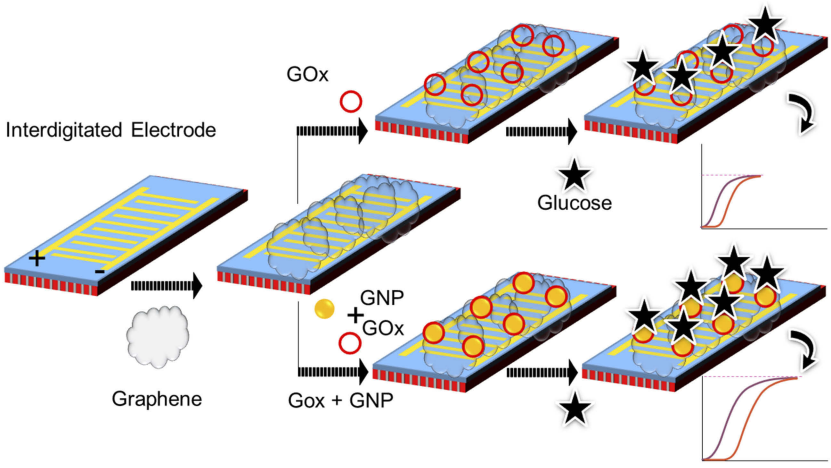

Figure 1 Schematic illustration for the dielectric sensing surface with the surface modifications. Surface modifications of GOx on graphene and GOx-GNP on graphene are shown for the comparison.
Abbreviations: GNP, gold nanoparticle; GOx, glucose oxidase.

microscopies. In addition, the nanocomposite formation was also observed on the silicon wafers. The preparation of graphene was followed by the exfoliation of graphite as outlined in our earlier study.[29] These observations are displayed in Figure 2A–E, based on the analysis by FESEM it was clear that the produced graphene materials have smoothened flakes. This structure was confirmed by the elemental identification by the energy dispersive X-Ray analyzer on the rastered FESEM image and FETEM observation (Figure 2B and C). Similarly, the intactness and uniformity of the GNP were studied by FETEM and found to be good with the expected averaged size of ~30 nm (Figure 2D). The formation of these graphene and gold nanocomposite was created by the chemical linker below and confirmed by FETEM. It was seen apparently that the nanocomposite formed was from the prepared graphene followed by the linked GNP (Figure 2E). The fabrication of IDE surface was followed based on our established method using the silicon as the basic substrate and the aluminum electrodes were formed on the silicon as the dielectric.[34,35] The fabricated IDE surface formed the clear finger and gap regions as observed under the SEM (Figure 3A).

Surface chemical functionalization: creation of nanocomposite

APTES was used extensively for this immobilization process to form the free amino groups on the surface of the IDE, further

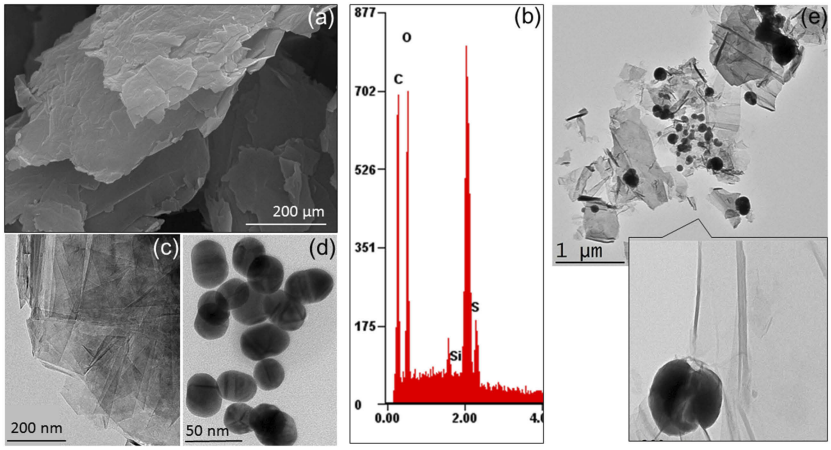

Figure 2 Surface morphology for nanoscale imaging. (**A**) FESEM observation for the graphene preparation; (**B**) Energy dispersive X-Ray analysis. The elemental compositions were found to confirm the presence of carbon; (**C**) FETEM observation for the graphene; (**D**) FETEM observation for the gold. The average size was measured to be 30 nm; (**D**) FETEM observation for the graphene-gold composite.
Abbreviations: FESEM, field-emission scanning electron microscopy; FETEM, field-emission transmission electron microscopy (FETEM).

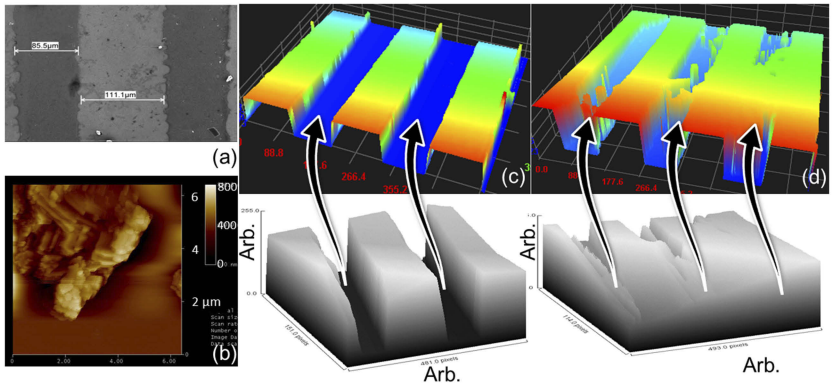

Figure 3 Surface morphology on IDE. (**A**) SEM observation for the surface of IDE; (**B**) AFM analysis on the graphene-modified IDE; (**C**) high-power microscopy-assisted 3D-nanoprofiler image for bare IDE; (**D**) high-power microscopy-assisted 3D-nanoprofiler image for molecules attached IDE. Both surfaces were compared by imageJ software scanning.
Abbreviations: IDE, interdigitated electrode; AFM, atomic force microscopy; SEM, scanning electron microscopy.

amine was used here to disperse the graphene on the IDE surface. The dispersion of graphene in the APTES leads to the binding of APTES and graphene, at the same time the unbound APTES also can bind on the surface of the IDE. It forms –Si-O-Si- (siloxane bond), it was created between the IDE surface and on the graphene, leads to the graphene-functionalized IDE surface. The attached graphene was confirmed by AFM analysis and clearly observed as in Figure 3B. The GOx was immobilized on the surface by crosslinking with the functional groups on the graphene. Eventually, the graphene-Gox complex was created on the IDE surface to detect the glucose. The same procedure used to create the surface of graphene-GOx-GNP on the IDE surface. The molecules attached surface was visualized by the high-power microscopy-assisted 3D-nanoprofiler and compared with the bare surface. Further support was rendered by the imageJ software-based analysis and could see the clear intensity differences between these surfaces (Figure 3C and D).

Analysis on dielectric IDE surface

The process of surface modification and immobilization on the IDE sensor was analyzed by the voltammetry analysis. Surface chemical analysis with FTIR has displayed predominantly C=C (aromatic), C-O (epoxy) and C-O (alkoxy) bonds (Figure 4A). Further analysis by zeta potential with graphene-GOx and graphene-GOx-GNP composite indicates to be −8.8 and −30.5 mV, respectively. The electrical measurements followed are shown in Figure 4B and C. The bare surface shows the current changes of $8.53E^{-08}$, and upon APTES modification with graphene, the current level was increased to $1.67E^{-06}$ (Figure 5A). This result confirms the attachment of graphene on the IDE surface and the remaining surface was blocked by 1 M ethanolamine with the current level increment to $2.88E^{-08}$. At the same time, the immobilization of graphene-GOx-GNP conjugates on the IDE sensing surface, the current level was increased from $8.51E^{-08}$ to 3.81^{-06} (Figure 5B). These changes with the current were higher than the surface of graphene alone, approximately two-fold enhancement with the graphene-GNP was noticed. This might be due to the higher number of GOx bound on the single GNP surface and immobilized on the IDE surface. When the ethanolamine was added, it shows the small changes in current due to the higher occupation of graphene-GNP conjugates on the IDE surface.

Detection of glucose on graphene-GOx and graphene-GOx-GNP modified dielectric surfaces: comparative analysis

To compare the detection of glucose on both graphene-GOx and graphene-GOx-GNP modified surfaces, 0.5 mg/mL of glucose was added on these surfaces after the surface blocked with ethanolamine. As shown in Figure 6A, on the graphene-GOx surface, there was a current decrement from $2.88E^{-06}$ to $1.63E^{-06}$. At the same time on the graphene-GOx-GNP modified surface, the current changes were noticed from $4.16E^{-08}$ to $1.17E^{-08}$ (Figure 6B). This shows ~2.5 times higher changes in current compared to graphene-GOx modified surfaces, due to the higher number on GOx binding on the graphene-GOx-GNP surface.

Sensitivity measurements on graphene-GOx and graphene-GOx-GNP modified dielectric surfaces

To check the limit of detection on both graphene-GOx and graphene-GOx-GNP modified surfaces, different

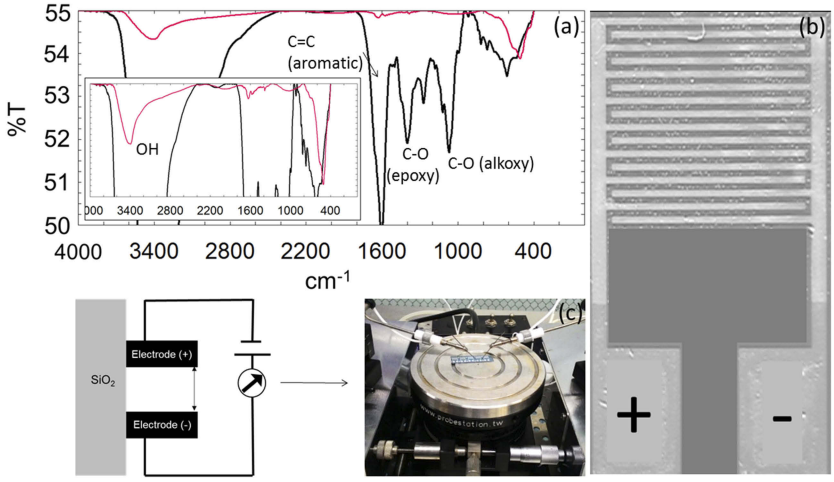

Figure 4 Surface chemical and electrical studies. (**A**) FTIR analysis. Graphene-GOx (black line) and graphene-GOx-GNP composite (red line) are shown. (**B**) Photograph of surface fabricated electrode. (**C**) Sensing methodology.
Abbreviations: FTIR, Fourier-transform infrared spectroscopy; GNP, gold nanoparticle; GOx, glucose oxidase; GNP, gold nanoparticle; GOx, glucose oxidase.

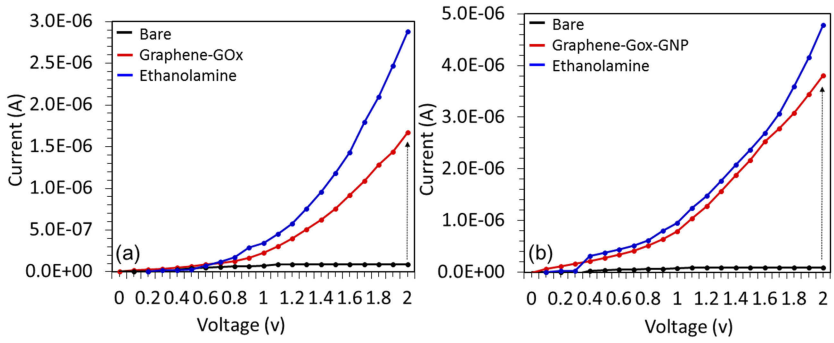

Figure 5 Comparative analysis between graphene-GOx and graphene-GOx-GNP surfaces by voltammetry measurements. The current variations from 0 to 2 V were utilized. Surfaces are (**A**) graphene-GOx and (**B**) graphene-GOx-GNP.
Abbreviations: GNP, gold nanoparticle; GOx, glucose oxidase.

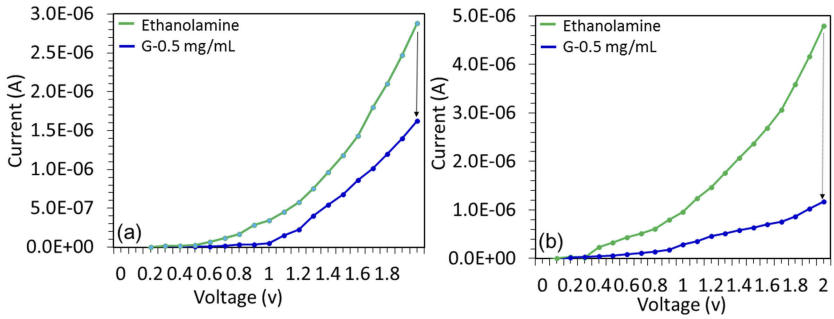

Figure 6 Comparative analysis between graphene-GOx and graphene-GOx-GNP surfaces for the interaction. The current variations from 0 to 2 V were utilized. After blocking by ethanolamine, 0.5 mg/mL of glucose was reacted with GOx. Surfaces are (**A**) graphene-GOx and (**B**) graphene-GOx-GNP.
Abbreviations: GNP, gold nanoparticle; GOx, glucose oxidase.

concentrations of glucose (0.03–0.5 mg/mL) were dropped on the prepared surfaces and the changes in the current were noted for comparison. Figure 7A displays different concentrations of glucose binding on graphene-GOx modified surface, it has been noticed that after the ethanolamine blocking 0.03 mg/mL of glucose did not show the changes in current, at the same time with increasing the concentrations further current changes were noted to be

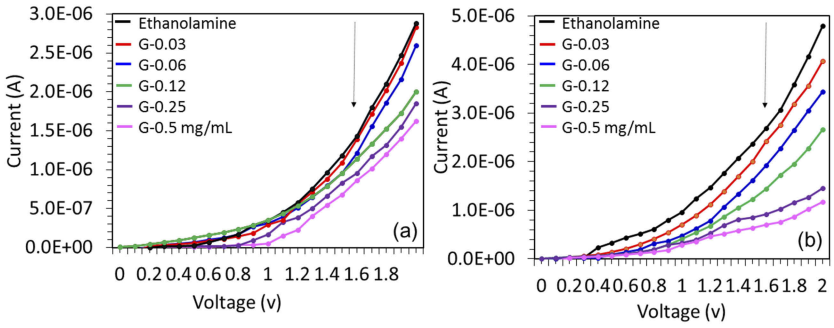

Figure 7 Sensitivity comparison between graphene-GOx and graphene-GOx-GNP surfaces for the interaction. The glucose concentrations from 0.03 to 0.5 mg/mL were tested and the sensitivity was calculated. Surfaces are (**A**) graphene-GOx and (**B**) graphene-GOx-GNP.
Abbreviations: GNP, gold nanoparticle; GOx, glucose oxidase.

gradually decreased. The current differences were noticed from ethanolamine as the baseline for the concentrations, 0.25, 0.12, 0.06 and 0.03 mg/mL as $0.29E^{-06}$, $0.87E^{-06}$, $1.03E^{-06}$ and $1.25E^{-06}$, respectively and the sensitivity was found as 0.06 mg/mL in this graphane surface. In the case, graphene-GOx-GNP modified surfaces the similar concentrations of glucose were dropped for the differentiation. It was found that 0.03 mg/mL of glucose showed a clear change of current from $4.16E^{-06}$ to $3.61E^{-06}$. With increasing the concentrations of the glucose, the current levels were gradually decreased as noted in the above case. The current differences were monitored from ethanolamine curve and measured for the concentrations, 0.25, 0.12, 0.06 and 0.03 mg/mL to be $0.72E^{-06}$, $1.42E^{-06}$, $2.71E^{-06}$ and $2.99E^{-06}$, respectively (Figure 7B). The sensitivity was found as 0.03 mg/mL and all the concentrations tested were displayed the higher level of current changes on the graphene-GOx-GNP modified surface compared to the graphene-GOx modified surface.

Linear regression analysis: limit of detection

With the above concentration-dependent analysis on graphene-GOx and graphene-GOx-GNP modified surfaces, the linear regressions were plotted. The limit of detection (LOD) was considered the lowest concentration of an analyte (from the calibration line at low concentrations) against the background signal (S/N=3:1), in other word, LOD=standard deviation of the baseline +3σ. The estimated LOD with graphene-GOx surface falls at 0.03 mg/mL, whereas graphene-GOx-GNP surface shows the LOD to be <0.03 mg/mL [0.02–0.03 mg/mL; Figure 8A and B]. This level of detection is lower than the normal human blood glucose level after the fasting. It has been generally proved that a normal human bloodstream maintains the glucose level to be 79–110 mg/dL with fasting.[36] The current detection with the detection lower than 0.03 mg/mL is highly reliable to monitor the blood sugar especially with the cases of the gestational diabetes mellitus. The obtained detection limit is comparable with the currently

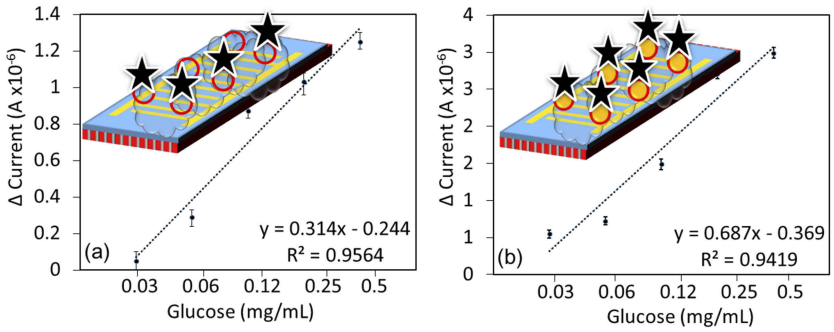

Figure 8 Linear regression analysis. 3σ estimation was followed. Surfaces are (**A**) graphene-GOx; (**B**) graphene-GOx-GNP. Figure insets display the different surface modifications.
Abbreviations: NP, gold nanoparticle; GOx, glucose oxidase.

available glucose sensing systems and shown the better performance (Table 1).

High-performance detection of glucose on graphene-GOx-GNP modified dielectric surface

To elucidate the high-performance detection on glucose on the graphene-GOx-GNP modified dielectric surface, specificity analyses were performed using different sugars. Lactose and fructose were chosen for interacting GOx and discriminated against the glucose reaction. With these three sugar molecules, GOx has shown the reaction only with the glucose and failed to detect other two sugars, indicates the high-performance detection without non-specificity (Figure 9A). Further, with all the above chemical and biological analyses data with multiple experiments were calculated for the error values with the standard deviation. With all the values, it was clear that the fabricated devices with different numbers have the similar output with minimal errors (Figure 9B). The stability of graphene-GOx and graphene-GOx-GNP was measured for 8 weeks at a week interval. The obtained measurements displayed the reduction of 10% activity at 6th and 7th weeks, respectively. After that, at 8th weeks in both cases ~50% loss in the stability was measured.

Table 1 Comparison of limit of detection with different glucose sensors

Sensor	Limit of detection	Ref.
Radio-frequency resonator	0.03 μM	7
Electrochemical sensor	0.1 mg/dL	10
Electrochemical sensor	0.5 mM	9
Nanoribbon transistor biosensor	10 nM	37
Electrochemical sensor	0.1 mM	38
Cryogel colorimetric	1 mM	39
Electrochemical sensor	50 μM	40
Cyclic voltammetry	1.5 mM	41
Optical fiber sensor	1 nM	42
3D-printed electrochemical sensor	6.9 μM	43
Electrochemical sensor	0.01 mM	44
Bioluminescence quenching	1 μM	45
Cyclic voltammetry	0.03 μM	46
Microcapillary biosensor	2.78 mM	47
Spectrophotometry	0.05 mg/mL	48
voltammetry	0.03 mg/mL	Current work

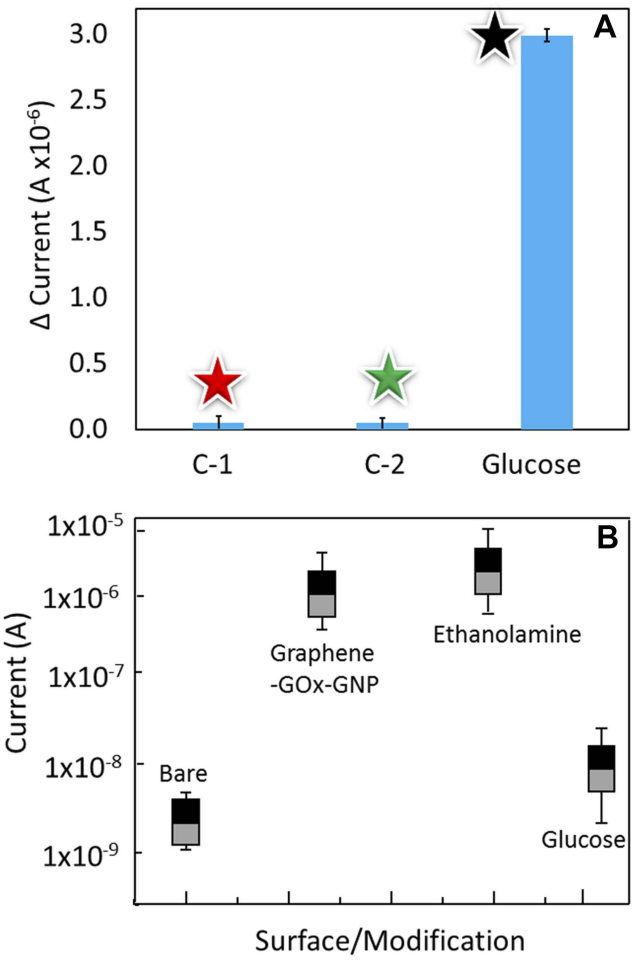

Figure 9 High-performance analysis. (**A**) Specificity analysis on glucose. Glucose and GOx reaction is indicated by the black star. Compared to the reaction of GOx with other sugars (lactose – C1 and Fructose –C2) marked by red and green stars, respectively. (**B**) Reproducibility analysis. Chemically and biologically modified surfaces where shown with the averaged values from different devices.
Abbreviations: NP, gold nanoparticle; GOx, glucose oxidase.

Conclusion

Gestational diabetes mellitus is a common disorder during the pregnancy period and a continuous blood glucose level monitoring is mandatory for the good health of mother and baby. To make the ideal sensing system with the high-performance and easier to operate, in this study graphene-modified gold impregnated nanocomposite dielectric surface has been made for the covalent immobilization of GOx. The surface was characterized for the interactive analyses with glucose (substrate) and attained the detection limit below 0.03 mg/mL, which is lower than the normal human blood glucose level during the fasting. High-performance of this nanocomposite surface was confirmed by the good sensitivity, specificity and reproducibility behavior. An ideal composition is with the above nanomaterial for

the bio- and chemical-molecular assembly demonstrated a good biosensor, to be suitable for other biomolecular interactions.

Disclosure

There are no conflicts of interest reported by the authors regarding this work.

References

1. Liu B, Xu Y, Zhang Y, et al. Early Diagnosis of Gestational Diabetes Mellitus (EDoGDM) study: a protocol for a prospective, longitudinal cohort study. *BMJ Open*. 2016;6:e012315. doi:10.1136/bmjopen-2016-012315
2. Spaight C, Gross J, Horsch A, et al. Gestational diabetes mellitus. *Endocr Dev*. 2016;26(suppl 1):s103–s105.
3. Berger H, Gagnon R, Sermer M, et al. Diabetes in pregnancy. *J Obstet Gynaecol Can*. 2016;38(7):667–679. doi:10.1016/j.jogc.2016.04.002
4. Utz B, Delamou A, Belaid L, et al. Detection and management of diabetes during pregnancy in low resource settings: insights into past and present clinical practices. *J Diabetes Res*. 2016;3217098.
5. Crowther CA, Hiller JE, Moss JR, et al. Effect of treatment of gestational diabetes mellitus on pregnancy outcomes. *Obstet Gynecol Surv*. 2005;352:2477–2486.
6. Diabetes P, Mellitus GD. Management of diabetes in pregnancy. *Diabetes Care*. 2016;38(Supplement1):S77–S79.
7. Kim NY, Adhikari KK, Dhakal R, et al. Rapid, sensitive, and reusable detection of glucose by a robust radiofrequency integrated passive device biosensor chip. *Sci Rep*. 2015;5:1–9.
8. Yusan S, Rahman MM, Mohamad N, et al. Development of an amperometric glucose biosensor based on the immobilization of glucose oxidase on the Se-MCM-41 mesoporous composite. *J Anal Methods Chem*. 2018;2687341.
9. Sharma S, Huang Z, Rogers M, et al. Evaluation of a minimally invasive glucose biosensor for continuous tissue monitoring. *Anal Bioanal Chem*. 2016;408(29):8427–8435. doi:10.1007/s00216-016-9961-6
10. Zhang W, Du Y, Wang ML. Noninvasive glucose monitoring using saliva nano-biosensor. *Sens Bio-Sensing Res*. 2015;4:23–29. doi:10.1016/j.sbsr.2015.02.002
11. Nagasaki Y. Construction of a densely poly(ethylene glycol)-chain-tethered surface and its performance. *Polym J*. 2011;43:949–958. doi:10.1038/pj.2011.93
12. Zhu Y, Murali S, Cai W, et al. Graphene and graphene oxide: synthesis, properties, and applications. *Adv Mater*. 2010;22:3906–3924. doi:10.1002/adma.201001068
13. Kemp KC, Georgakilas V, Otyepka M, et al. Functionalization of graphene : covalent and non-covalent approaches, derivatives and applications. *Chem Rev*. 2012;112(11):6156–6214. doi:10.1021/cr3000412
14. Liu Y, Dong X, Chen P. Biological and chemical sensors based on graphene materials. *Chem Soc Rev*. 2012;41:2283–2307. doi:10.1039/c1cs15270j
15. Kakaei K, Esrafili MD, Ehsani A. Graphene-based electrochemical supercapacitors. *Interface Sci Technol*. 2019;27:339–386.
16. Wang Y, Li Y, Tang L, Lu J, Li J. Application of graphene-modified electrode for selective detection of dopamine. *Electrochem Commun*. 2009;11(4):889–892. doi:10.1016/j.elecom.2009.02.013
17. Luo J, Jiang S, Zhang H, Jiang J, Liu X. A novel non-enzymatic glucose sensor based on Cu nanoparticle modified graphene sheets electrode. *Anal Chim Acta*. 2012;709(4):47–53. doi:10.1016/j.aca.2011.10.025
18. Stankovich S, Dikin DA, Dommett GHB, et al. Graphene-based composite materials. *Nature*. 2006;442:282–286. doi:10.1038/nature04969
19. Lv Q, Wang Y, Su C, et al. Human papilloma virus DNA-biomarker analysis for cervical cancer: signal enhancement by gold nanoparticle-coupled tetravalent streptavidin-biotin strategy. *Int. J. Biol. Macromol.* 2019;186:336. doi:10.1016/j.exer.2019.107700
20. Lakshmipriya T, Gopinath SCB, Tang T-H. Biotin-streptavidin competition mediates sensitive detection of biomolecules in enzyme linked immunosorbent assay. *PLoS One*. 2016;11:e0151153. doi:10.1371/journal.pone.0151153
21. Lakshmipriya T, Horiguchi Y, Nagasaki Y. Co-immobilized poly(ethylene glycol)-block-polyamines promote sensitivity and restrict biofouling on gold sensor surface for detecting factor IX in human plasma. *Analyst*. 2014;139(16):3977–3985. doi:10.1039/C4AN00168K
22. Uchida K, Otsuka H, Kaneko M, Kataoka K, Nagasaki Y. A reactive poly(ethylene glycol) layer to achieve specific surface plasmon resonance sensing with a high S/N ratio: the substantial role of a short underbrushed PEG layer in minimizing nonspecific adsorption. *Anal Chem*. 2005;77(4):1075–1080. doi:10.1021/ac0486140
23. Altintas Z. Surface plasmon resonance based sensor for the detection of glycopeptide antibiotics in milk using rationally designed nanoMIPs. *Sci Rep*. 2018;8:11222. doi:10.1038/s41598-018-29585-2
24. Gopinath SCB, Awazu K, Fujimaki M, et al. Observations of immuno-gold conjugates on influenza viruses using waveguide-mode sensors. *PLoS One*. 2013;8:1–10. doi:10.1371/annotation/7bb0ff7b-3527-4a42-a50a-ec81f108ac41
25. Chung E, Gao R, Ko J, et al. Trace analysis of mercury(II) ions using aptamer-modified Au/Ag core-shell nanoparticles and SERS spectroscopy in a microdroplet channel. *Lab Chip*. 2013;13:260–266. doi:10.1039/c3lc50269d
26. Shiota M, Naya M, Yamamoto T, et al. Gold-nanofève surface-enhanced Raman spectroscopy visualizes hypotaurine as a robust anti-oxidant consumed in cancer survival. *Nat Commun*. 2018;9:1561.
27. Brosel-Oliu S, Galyamin D, Abramova N, et al. Impedimetric label-free sensor for specific bacteria endotoxin detection by surface charge registration. *Electrochim Acta*. 2017;243(20):142–151. doi:10.1016/j.electacta.2017.05.060
28. Zarei SS, Soleimanian-Zad S, Ensafi AA. An impedimetric aptasensor for Shigella dysenteriae using a gold nanoparticle-modified glassy carbon electrode. *Microchim Acta*. 2018;185(12):538. doi:10.1007/s00604-018-3075-0
29. Gopinath SCB, Anbu P, Theivasanthi T, et al. Characterization of reduced graphene oxide obtained from vacuum-assisted low-temperature exfoliated graphite. *Microsyst Technol*. 2018;24(12):5007–5016. doi:10.1007/s00542-018-3921-3
30. Letchumanan I, Md Arshad MK, Balakrishnan SR, et al. Gold-nanorod enhances dielectric voltammetry detection of c-reactive protein: a predictive strategy for cardiac failure. *Biosens Bioelectron*. 2019;130:40–47. doi:10.1016/j.bios.2019.01.042
31. Guo S, Lakshmipriya T, Gopinath SCB, et al. Complementation of ELISA with interdigitated electrode surface in gold nanoparticle functionalization for effective detection of human blood clotting defect. *Nanoscale Res Lett*. 2019;14:222. doi:10.1186/s11671-019-3058-z
32. Perumal V, Saheed MSM, Mohamed NM, et al. Gold nanorod embedded novel 3D graphene nanocomposite for selective bio-capture in rapid detection of Mycobacterium tuberculosis. *Biosens Bioelectron*. 2018;116:116–122. doi:10.1016/j.bios.2018.05.042
33. Zheng D, Vashist SK, Dykas MM, et al. Graphene versus multi-walled carbon nanotubes for electrochemical glucose biosensing. *Materials (Basel)*. 2013;6(3):1011–1027. doi:10.3390/ma6031011
34. Letchumanan I, Gopinath SCB, Md Arshad MK, et al. Gold nano-urchin integrated label-free amperometric aptasensing human blood clotting factor IX: a prognosticative approach for "Royal disease.". *Biosens Bioelectron*. 2019;131:128–135. doi:10.1016/j.bios.2019.02.006
35. Wang H, Lakshmipriya T, Chen Y, et al. Squamous cell carcinoma biomarker sensing on a strontium oxide-modified interdigitated electrode surface for the diagnosis of cervical cancer. *Biomed Res Int*. 2019;2019:1–7. doi:10.1155/2019/8023541

36. Gray LJ, Davies MJ, Khunti K. Screening for type 2 diabetes. *Controv Obes*. 2014;27(supp 1):s11–s14.
37. Liu Q, Liu Y, Wu F, et al. Highly sensitive and wearable in 2 O 3 nanoribbon transistor biosensors with integrated on-chip gate for glucose monitoring in body fluids. *ACS Nano*. 2018;12(2):1170–1178. doi:10.1021/acsnano.7b06823
38. Bollella P, Sharma S, Cass AEG, et al. Minimally invasive glucose monitoring using a highly porous gold microneedles-based biosensor: characterization and application in artificial interstitial fluid. *Catalysts*. 2019;9(7):580. doi:10.3390/catal9070580
39. Fatoni A, Dwiasi DW, Hermawan D. Alginate cryogel based glucose biosensor. *IOP Conf Ser Mater Sci Eng*. 2016;107:012010. doi:10.1088/1757-899X/107/1/012010
40. Su S, He Y, Song S, et al. A silicon nanowire-based electrochemical glucose biosensor with high electrocatalytic activity and sensitivity. *Nanoscale*. 2010;2:1704–1707. doi:10.1039/c0nr00314j
41. Rodrigues A, Castegnaro MV, Arguello J, et al. Development and surface characterization of a glucose biosensor based on a nanocolumnar ZnO film. *Appl Surf Sci*. 2017;402:136–141. doi:10.1016/j.apsusc.2017.01.052
42. Yin M, Huang B, Gao S, et al. Optical fiber LPG biosensor integrated microfluidic chip for ultrasensitive glucose detection. *Biomed Opt Express*. 2016;7(5):2067–2077. doi:10.1364/BOE.7.002067
43. Nesaei S, Song Y, Wang Y, et al. Micro additive manufacturing of glucose biosensors: a feasibility study. *Anal Chim Acta*. 2018;1043:142–149. doi:10.1016/j.aca.2018.09.012
44. Wei A, Sun XW, Wang JX, et al. Enzymatic glucose biosensor based on ZnO nanorod array grown by hydrothermal decomposition. *Appl Phys Lett*. 2006;89:123902. doi:10.1063/1.2356307
45. Chen L, Chen L, Dotzert M, et al. Nanostructured biosensor using bioluminescence quenching technique for glucose detection. *J Nanobiotechnology*. 2017;15:59. doi:10.1186/s12951-017-0305-2
46. Norouzi P, Faridbod F, Larijani B, et al. Glucose biosensor based on MWCNTs-gold nanoparticles in a nafion film on the glassy carbon electrode using flow injection FFT continuous cyclic voltammetry. *Int J Electrochem Sci*. 2010;5(2010):1213–1224.
47. Wan H, Chen J, Wan C, et al. Optofluidic microcapillary biosensor for label-free, low glucose concentration detection. *Biomed Opt Express*. 2019;10(8):3929. doi:10.1364/BOE.10.003929
48. Lopes FM, Batista KDA, Batista GLA, et al. Biosensor for determination of glucose in real samples of beverages. *Food Sci Technol*. 2012;32(1):65–69. doi:10.1590/S0101-20612012005000003